General Analytical Solution for Estimating the Elastic Deformation of an Open Borehole Wall

Asad Elmgerbi, Gerhard Thonhauser, Michael Prohaska, Abbas Roohi and Andreas Nascimento

Abstract—Few analytical solutions have been published in the past decades for quantifying the ballooning volume caused by elastic deformation of an open borehole; nevertheless none of them takes into consideration the effects of permeability and thermoelasticity. This paper introduces new analytical solutions aiming at predicting a radial elastic displacement for any point along an open borehole wall. The presented analytical formulas here are general and taking into account the effective stresses, thermoelasticity and the poroelasticity effects. Two analytical formulas are derived, one for impermeable borehole, whereas the second is for permeable borehole. To utilize the proposed analytical solution for estimation the volumetric expansion and contraction of an open borehole, a recognized mathematical method has been adapted to be used for defining the areal elastic deformation of an open borehole at a given depth, which later can be used to quantify the volumetric change of an open borehole for specified depth interval. In order to validate the proposed formulas a finite element simulation was utilized. Several cases have been examined and compared, generally good results were observed with relative error less than 15%. Finally, results of a sensitivity study which was performed in order to assess the effects of different parameters on volumetric deformation of the open borehole are presented and discussed in details, the main finding of this study was that the deformation area of the borehole due to the elastic deformation is not significant and controlled mainly by the wellbore pressure.

Index Terms—Elastic deformation, thermoelasticity, effective stresses, Biot elastic constant, grain bulk modulus, ABAQUS, poroelasticity.

1 INTRODUCTION

ACCURATE detection of drilling problems, without a doubt, it is an important moment during drilling operations. In drilling, thus far, there are problems, which are still complex to be recognized and classified. One of these problems is borehole ballooning or breathing.
Borehole ballooning or breathing is a phenomenon, which can be described as the reversible process of active drilling fluid volume gain and loss during drilling operations. It is very crucial to understand the major mechanisms and factors controlling the ballooning phenomenon to avoid confusion with conventional losses or formation kick. Therefore misinterpretation of the consequences of this phenomenon can lead eventually to excessive non-productive time. So far five processes are known as the main causes of the borehole ballooning, they can be categorized as following [1 & 2]:

- Drilling fluid related processes:
  - Thermal expansion and contraction of the drilling fluid due to change in system temperature.
  - Compression and expansion of the drilling fluid due to change in wellbore pressure.
- Wellbore related processes:
  - Elastic deformation of the borehole and the cased hole.
  - The opening and closing of induced fractures at the near wellbore region.
  - The opening and closing of natural fractures [pre-existing] intersected during drilling.

Fig. 1 illustrates the main causes of the borehole ballooning.

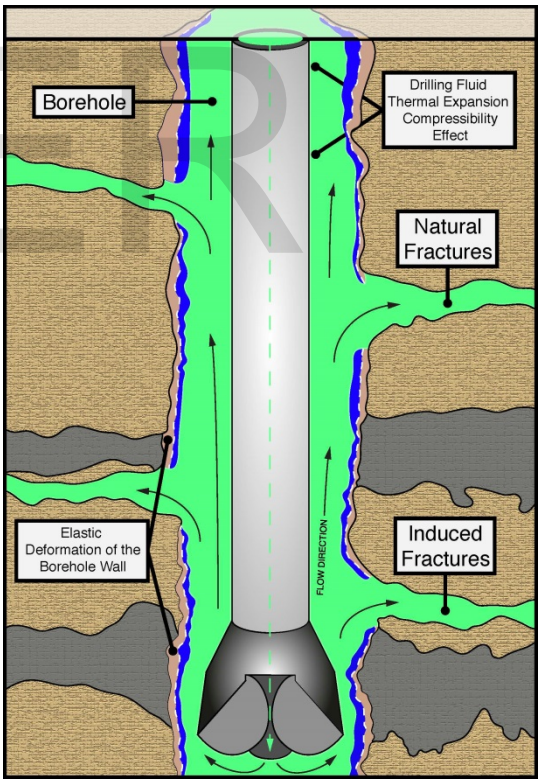

Fig 1. The Main Causes of the Borehole Ballooning.

The first analytical solution used to calculate the displacements around a circular excavation was published by Kirsch (1898); although his solution is quite old, it is still useful for tunneling design.

Gill (1989) identified the elastic deformation of the borehole wall due to pressure changes as the main driver of this phenomenon [3]. Bjørkevoll et al (1994) and Aadnøy (1996) studied two contributors to borehole ballooning, drilling fluid expansion and contraction and the elastic deformation of borehole and casing. They came up with the following conclusion: the change in volume of the wellbore was mainly governed by the expansion and the contraction of the drilling fluid [4].

Kårstad and Aadnøy (1996-1997) presented a method for calculating the elastic deformation of the borehole wall in order to estimate the variation in volume of the wellbore. They did not consider the in situ stresses in their method. Moreover they did not use proper rock properties such as Young's modules [5].

In (2001) Helstrup et al, introduced an analytical formula for computing radial diametrical displacement of the borehole wall, they superimposed two equations, one for inward displacement and a second for outward displacement. In order to validate their analytical solution, they compared the results of their analytical solution with a numerical solution [5]. In essence their solution has significant shortcomings, which can be summarized as following:

- They did not use realistic models for their comparisons; the models should be two dimensional for better comparisons.
- The used numerical models for the comparisons did not take into account the poroelasticity theory.
- They assumed that the deformable areas have perfect elliptical shape.
- Their solution ignored the shear stresses.

Recently, Al-Tahini et al (2008) performed experimental studies in order to identify a correlation between the far field stresses with introduced stresses, displacement and breakout stresses. Based on their presented work the following shortcomings can be drawn [6]:

- They used uniaxial stresses and applied isotropic stresses.
- Poroelasticity was ignored.
- They considered the rocks as block (zero porosity) in the finite element simulation whereas at the lab they used rocks with porosity.

The shortcomings which were mentioned in the foregoing were the main motivations for deriving the new analytical formulas. The proposed analytical formulas are initially used to compute the radial diametrical elastic deformation of an open borehole wall. Furthermore, the paper introduces an accurate method for calculating the area of the deformation of the borehole wall which in turn can be used to estimate the ballooning volume. The main objective of the sensitivity study, presented at the end of the paper, is to individually determine the influences of different parameters on elastic deformation of an open borehole.

2 Theory and Mathematical Derivation of the Solutions

2.1 Basic Assumptions

The following assumptions are the essential and basic for deriving the solutions, the advanced assumptions will be listed later beside the derivations.

- Homogeneous and isotropic rock properties.
- Consolidated rock.
- Void space is fully saturated with one fluid.
- Normal faulting regime,
- An isotropic stress state exists.
- The in-situ stress state has three known principal stresses.
- The shear stresses are non-zero for arbitrary orientations of the borehole after the transformation.
- Gravity force is excluded.
- Plane strain status exists.

2.2 Essential Steps

The linear equation governing the normal stress/strain relation (Hooke's law) in one dimension was the starting point for the derivations.

$$\sigma = E * \varepsilon \tag{1}$$

$$\varepsilon = \sigma / E \tag{2}$$

Assuming isotropic rock materials, the normal stress/strain equations in three dimensional Cartesian coordinate system (x, y, z) can be written as the following matrix [7]:

$$\begin{bmatrix}\varepsilon_x\\ \varepsilon_y\\ \varepsilon_z\end{bmatrix} = \frac{1}{E} * \begin{bmatrix}1 & -\upsilon & -\upsilon\\ -\upsilon & 1 & -\upsilon\\ -\upsilon & -\upsilon & 1\end{bmatrix} * \ * \begin{bmatrix}\sigma_x\\ \sigma_y\\ \sigma_z\end{bmatrix} \tag{3}$$

However when converted to cylindrical coordinates (r, θ , z), its matrix will have the following form:

$$\begin{bmatrix}\varepsilon_r\\ \varepsilon_\theta\\ \varepsilon_z\end{bmatrix} = \frac{1}{E} * \begin{bmatrix}1 & -\upsilon & -\upsilon\\ -\upsilon & 1 & -\upsilon\\ -\upsilon & -\upsilon & 1\end{bmatrix} * \begin{bmatrix}\sigma_r\\ \sigma_\theta\\ \sigma_z\end{bmatrix} \tag{4}$$

Radial displacement for a cylindrical coordinates can be computed using the following sequences:

$$\varepsilon_\theta = \frac{\Delta \text{ Circumference}}{\text{Circumference}} \tag{5}$$

$$\varepsilon_\theta = \frac{2 * \pi * (r + u) - 2 * \pi * r}{2 * \pi * r} \tag{6}$$

$$\varepsilon_\theta = \frac{u}{r} \tag{7}$$

$$u = \varepsilon_\theta * r \tag{8}$$

While drilling, the periodic expansion and contraction in the borehole wall are expected within the elastic reign. Thus, the radial displacement at any point along an open borehole is variable and depending on multiple parameters. It is a positive number in expansion case and a negative number in con-

traction case.

2.3 General Elastic Solution for Impermeable Borehole Wall

In the following paragraphs only the important steps and equations will be explained. Thus, for more details, refer to Appendix [A]. According to Eq. 8 the tangential strain is the interesting strain which will be used for calculating the radial displacement. Therefore the derivation starts from the tangential strain formula (Eq. A2). As mentioned earlier, the input stresses must be the principal in-situ stresses. Since the wellbore may take any orientation and azimuth, these stresses are to be transformed to a new Cartesian coordinate system (x^0, y^0, z^0), where two stresses be perpendicular to the borehole whereas the third stress be parallel to the axes of the borehole. The three new stresses, σ_x° , σ_y° and σ_z° can be determined using Eqs. A4, A5 and A6, respectively. The directions and the magnitudes of the new stress components are given by the wellbore inclination from vertical and azimuth [7].

For simplicity the following notations are used for vertical and deviated borehole, σ_H, σ_h, and σ_v, instead of σ_x°, $\sigma_y^\circ$and σ_z° respectively. Once the stresses transformed and new stress components are obtained, the stress distribution around a borehole located in an arbitrary far-field stress field can be estimated using Bradley (1979) equations [8]. [See Eqs A10 to A13]

Next step is to apply the advanced assumptions and considerations to Eqs. A10, A11, A12 and A13;

- Since predicting the radial displacement at the borehole radius is the target [R=r].
- Considering the effective stress concept by including formation pore pressure.
- Taking into consideration poroelasticity theory by using Biot elastic constant.
- Concerning thermoelasticity by including thermal stress.
- The rock formation has a constant pore pressure (impermeable borehole wall & there is no communication between borehole pressure and formation pressure).

The resultant stresses after applying the advanced assumptions and considerations are effective stresses. The tangential strain formula (Eq. A2) can be rewritten by replacing σ_r , σ_θ and σ_z with Eqs. A14, A15 and A16 respectively, finally the tangential strain at any point along the borehole wall is computed as seen in Eq. A20. Bear in mind that the computed tangential strain in Eq. A20 considers the displacement towards the borehole center as positive displacement. Therefore the sign of the computed tangential strain in Eq. A20 must be changed, so that the outward displacement becomes positive [expansion].

$$u = (-) * \varepsilon_\theta * r \tag{9}$$

Finally the proposed formulas for computing the radial elastic displacement of an impermeable borehole wall is obtained by substituting tangential strain in Eq. 9 by Eq. A20.

$$u = r * \frac{(1+\upsilon)}{E}\left[P_w - \frac{(2\upsilon-1)}{(1+\upsilon)} * \left(B * P_p\right) - \frac{(1-\upsilon)}{(1+\upsilon)} * \sigma_t^{\Delta t} - \frac{1}{(1+\upsilon)} * (\sigma_H + \sigma_h - \upsilon * \sigma_v) - 2 * (\upsilon - 1) * \left((\sigma_H - \sigma_h)\,COS(2\theta) + 2 * \tau_{xy} * SIN(2\theta)\right)\right] \tag{10}$$

2.4 General Elastic Solution for Permeable Borehole Wall

The following points summarize the derivation steps;

- Earlier mentioned basic assumptions are necessary.
- Derivation starts from Eq. A2.
- A term called swelling effect is considered, it adds an additional compressive stress to tangential and axial stresses [9].
- Applying the advanced assumptions and considerations.
- Because the borehole wall is permeable, the formation pore pressure is changed by communication with the borehole pressure.
- After a certain time, the filter cake is built and consequently the steady state condition is reached and the formation pore pressure at the borehole vicinity will equal the borehole pressure. Thus borehole pressure must be used rather than formation pore pressure when computing the effective stresses.
- Insert the effective stresses Eqs. B1, B2 and B3 into Eq. A2.
- The tangential strain formula is established (Eq. B5).
- Eventually the analytical solution for obtaining the radial elastic displacement of a permeable borehole wall within the elastic deformation zone can be obtained by replacing the tangential strain in Eq. 9 with Eq. B5. All tables and figures will be processed as images. You need to embed the images in the paper itself. Please don't send the images as separate files.

$$u = r * \frac{1}{E}\left[P_w * (1+\upsilon) - (B * P_w) * (2\upsilon - 1) - (1-\upsilon) * \left(\sigma_t^{\Delta t} + 2\eta\left(P_w - \left(B * P_p\right)\right)\right) - (\upsilon^2 - 1) * \left(2(\sigma_H - \sigma_h)\,COS(2\theta) + 4 * \tau_{xy} * SIN(2\theta)\right) - \sigma_H - \sigma_h + \upsilon * \sigma_v\right] \tag{11}$$

Refer to Appendix [B] for more details.

3 Volume of Elastically Deformed Borehole Estimation Approach

3.1 General Overview

Focusing on a transverse section of an open borehole at a particular depth, when the borehole is deformed, the new shape of the borehole will not be uniform; however it will vary with the position around the borehole. According to the presented analytical solutions, two factors are responsible for having irregular shape. First factor, or the main dominator is the anisotropic in-situ stresses (maximum and minimum horizontal

stresses), whereas the second factor is one of the shear stresses (τ_{xy}), which is in fact governed by borehole position (azimuth and inclination). In the best case when the borehole is vertical only the former factor exists and the shape of the deformed borehole will be perfectly elliptic. In general the unusual shapes are always expected. Therefore it was necessary to determine a systematic and comprehensive method which can be used to accurately compute the difference in cross section area [deformation area] between the original borehole shape and the deformed borehole shape at a particular planar and depth. Once the difference in the cross section area is obtained the shortage or the excess in volume of the borehole for a desirable depth interval can be estimated.

3.2 Mathematical Description of the Method

As it is obvious in Eqs. 10 and 11 the computed radial elastic displacements of the borehole wall considerably depend on the angle theta (θ), which represents the central angle of the borehole measured anticlockwise from the azimuth of maximum horizontal stress (σ_H)[5]. Fig. 2 shows the angle theta (θ).

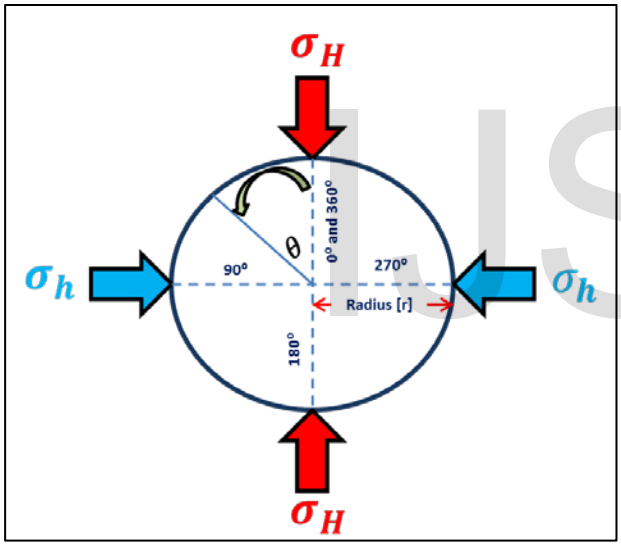

Fig 2. Angle Theta (θ) Direction and Starting Point (Transverse Cross Section View).

As it can be seen from Fig. 2, the angle theta (θ) starts from zero degree and increases along the circumference of the borehole till it gets back to the starting point. In mathematics, an arc of a circle is a portion of the circumference of the circle. The length of an arc is simply the length of its portion of the circumference. Actually, the circumference itself can be considered an arc length. The formula for measuring the length of an arc of a circle is:

$$\text{Arc Length} = \frac{\pi * \text{Radius of the circle} * \text{Central angle in degrees}}{180} \quad (12)$$

By comparing Fig. 2 with Eq. 12 one can come up with the following fact; borehole radius and angle theta (θ) are corresponding to radius of the circle and central angle respectively. Therefore Eq.12 can be used to compute the arc length along the borehole perimeter for each angle theta (θ) starting from 0^0 to 360^0. Now Eq.12 can be rewritten as outlined below:

$$\text{Arc Length} = \frac{\pi * \text{Initial radius of borehole} * \text{Angle theta in degree}}{180} \quad (13)$$

3.3 Identifying the Deformation Area and Computing the Volumetric Change

Calling back the radial elastic displacement Eqs. 10 and 11, as it explained in the previous section those equations are valid only if deformation occurs to the borehole wall and they are used to predict the radial elastic displacement along the circumference of the borehole for a given depth, where only angle theta (θ) is variable. In order to identify deformation area, the arc length of the virgin borehole must be coupled with the radial elastic displacement of the borehole wall after deformation. The only variable which is in common between the arc length of the virgin borehole and radial elastic displacement of the borehole wall is angle theta (θ). In other words for each angle there are specific arc length and radial elastic displacement. Let's now plot arc length in [x] axis (computed by Eq. 13) versus corresponding radial elastic displacement in [y] axis (calculated by either Eq. 10 or 11) for a complete cycle of the angle theta (θ) starting from [0^0] to [360^0] by [1^0] increment. Fig. 3 illustrates the inclusive summary.

From Fig. 3 one can conclude the following points:

- The positive displacements are identical representative to the borehole expansion.
- The negative displacements are identical representative to the borehole contraction.
- The areas under the curves in Fig. 3 are the deformation areas.
- The total deformation area is equal to the sum of the areas under the curves.

Based on the points outlined above the total deformation area for a given depth can be predicted only if the area under each curve is individually estimated. Therefore it was necessary to define a method which can easily calculate the area under the curve. Several methods are used to estimate the area under the curve one of this method is Riemann sum [10].

By employing this method, first we divide the area under the curve into small rectangles, then we calculate the area of the each rectangle individually, afterwards the total deformation area can be estimated by adding up all the calculated areas of the rectangles.

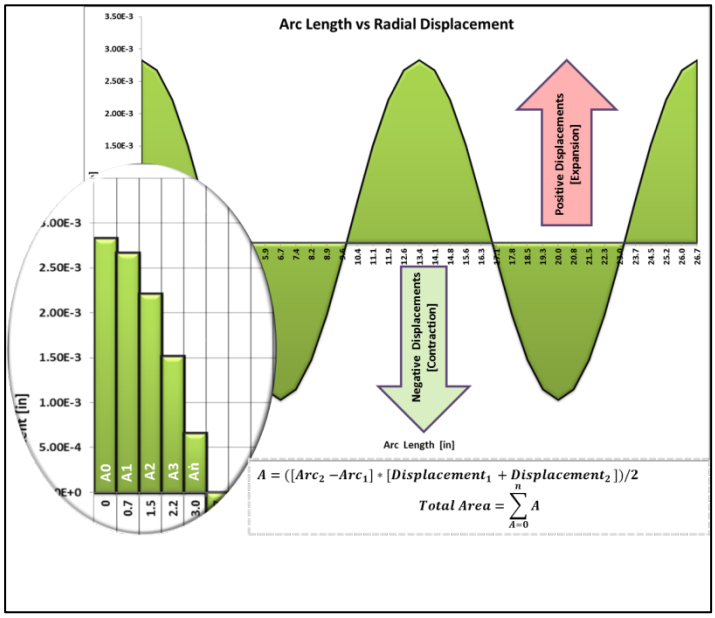

Fig 3. Arc length vs Radial Elastic Displacement Plot [for Specific Depth] to Define the Total Deformation Area.

The resulting deformation area of this process can be used to estimate the volumetric change due to elastic deformation for one increment in depth [Deformation volume].

$$\text{Deformation volume} = \text{Total Deformation Area} * \text{Desirable (increment in) depth} \quad (14)$$

The same process must be repeated for each increment in depth. Finally the summation of deformation volumes will result in the total volumetric change of the open borehole interval. Once more, the total volumetric change of the open borehole interval might be negative or positive number, negative number indicates to contraction in the borehole and consequently excessive return drilling fluid at the surface is expected. However the positive number is the sign of the expansion in the borehole, which leads to loss more drilling fluid to fill the gap. Fig. 4 presents the outline to identify the total volumetric change of the open borehole interval due to elastic deformation, for better illustration.

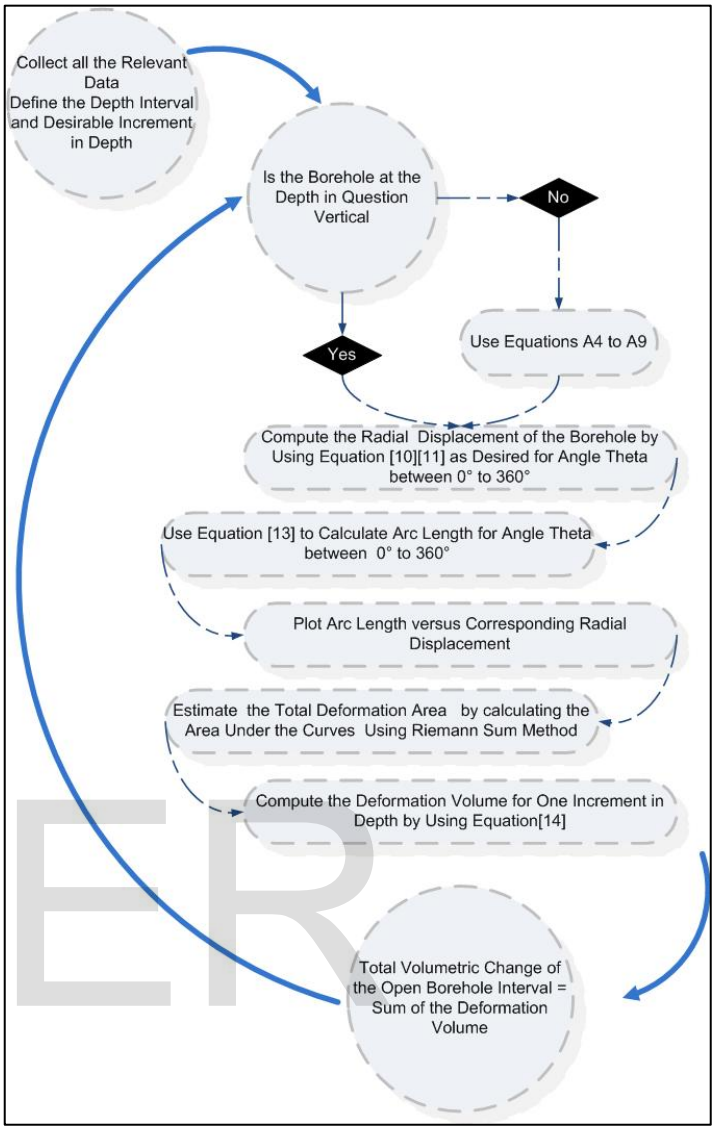

Fig 4. Workflow to Identify the Total Volumetric Change of the Open Borehole Interval Due to Elastic Deformation.

4 Solutions Validation

Finite element simulations were performed to validate the proposed analytical solutions using ABAQUS. Two models were constructed. Several cases were examined. Data related to radial elastic displacement along the perimeter of the borehole in all cases were extracted subsequently the total deformation area for each case was calculated by using similar method to the one used to estimate the total deformation area in the analytical solutions. Finally, the relative error was used as a key performance indicator in order to measure the strength of the relation between the numerical and analytical solutions. Length and width of the used model and the model after applying the mesh is shown in Fig. 5.

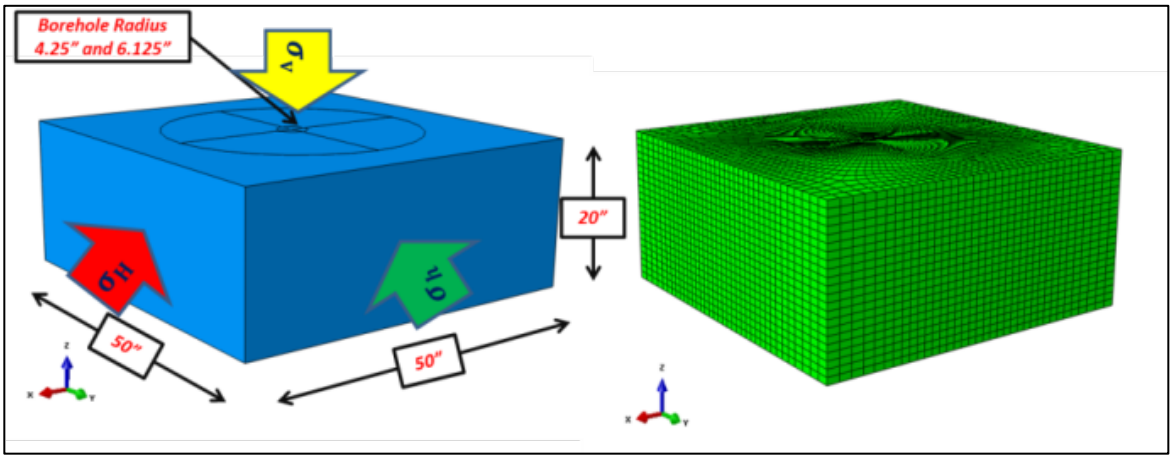

Fig 5. Geometry of the Models and Stresses Deployment

4.1 Poroelasticity Implementation

Applying poroelasticity theory in ABAQUS requests to identify a relation between Biot elastic constant [α] and the rock properties. The Biot elastic constant of a rock is an important poroelastic parameter that relates stresses and formation pore pressure, it measures the ratio of the fluid volume squeezed out to the volume change of the rock if the latter is compressed while allowing the fluid to escape. Being described as [11];

$$\alpha = 1 - \frac{\text{Frame bulk modulus}}{\text{Grain bulk modulus}} \quad (15)$$

$$\text{Frame Bulk Modulus} = \frac{\text{Young's modulus}}{3 * (1 - 2 * \text{Poisson ratio})} \quad (16)$$

By knowing Biot elastic constant and frame bulk modulus the grain bulk modulus can be calculated and used. Several equations were suggested to estimate the Biot elastic constant only by using the rock porosity. The strength of discrepancy between those equations is very high at low porosity and vice versa. In addition to the mathematical equations an experimental work was performed by Detournay and Cheng (1993) to define the relation between Biot elastic constant and rock porosity and then the mathematical and experimental Biot elastic constant versus porosities were plotted. Consequently the best correlation was established and the following equation was recommended [12]:

$$\alpha = \frac{P * \emptyset^{q}}{1 + \emptyset} \quad (17)$$

(P) and (q) are constant values and they vary with the rock type. In order to assign one porosity for a given Biot elastic constant, first we calculate the porosity using the equations listed in Appendix [C]. The second step is to assume initial values to two constants (P) and (q), because only one Biot elastic constant exists every time. Therefore the third step is to define the actual values of the two constants by using Eq. 17 for all the pre-calculated porosities in conjunction with one of the available statistical tools such as Oracle Crystal Ball. Finally, by knowing the two constants and Biot elastic constant the best corresponding porosity can be calculated by using Eq. 17.

4.2 Models Setup

The models were set in a manner that all the basic and advanced assumptions have been implemented. In order to simulate the real conditions, the model was initially constructed without borehole, the stresses were first applied then the borehole was introduced and borehole pressure was applied. As it was explained earlier the poroelasticity was implemented by introducing porosity, grain bulk modulus, fluid bulk modulus and permeability, for simplicity water was used as fluid media, porosity and permeability were kept constant, fluid specific weight was defined based on the applied formation pore pressure. Pore fluid and stress element with eight nodes type was used. To guarantee constant formation pore pressure for entire simulation running time, a formation pore pressure boundary condition was defined. For permeable borehole wall model, an additional formation pore pressure boundary condition is applied at the borehole wall. Additional boundary conditions were needed to prevent any displacement/deformation of initial model from applied loads. Fig. 6 shows the model with the main boundary conditions.

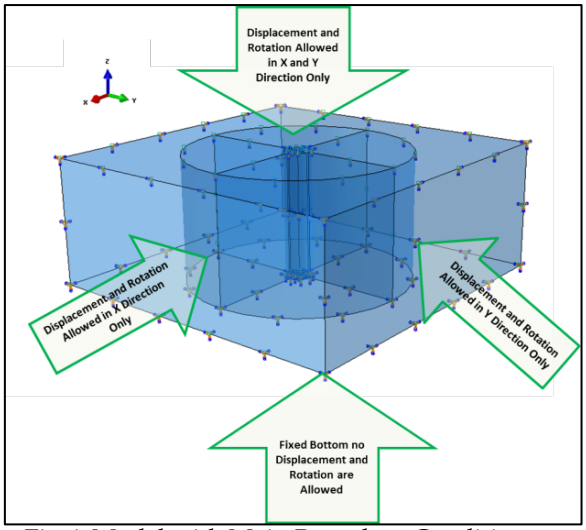

Fig 6. Model with Main Boundary Conditions.

4.3 Results and Comparisons

Results of finite element (numerical) analysis have been used to verify the analytical solutions proposed for elastic deformation of open boreholes. Table 1 presents the input data used in ABAQUS for all examined cases. The comparison between analytical solution results and simulation results in terms of total deformation area and relative error is illustrated in Table 2. From Table 2 it is observed that the relative errors are less than 15% which indicates good match between the two solutions. Thus the analytical solutions proposed in this paper for elastic deformation give reasonably accurate results.

Input Data						
Case	1	2	3	4	5	6
Depth [ft]	3000	3000	6000	5000	5000	12000
Borehole Radius [in]	4.25	4.25	4.25	6.125	6.125	4.25
Vertical Stress [psi]	3300	3300	6000	5500	5500	5500
Max Horizontal Stress [psi]	2850	2850	5640	4750	4750	4750
Min Horizontal Stress [psi]	2400	2400	4200	4000	4000	4250
Formation Pore Pressure [psi]	1320	1320	3480	2200	2200	2250
Applied Borehole Pressure [psi]	2950	1838	4662	4920	2860	3731
Young's Modulus [psi]	1450326	1450326	2273416	1740391	1740391	2175489
Poisson's Ratio	0.35	0.35	0.3	0.4	0.4	0.35
Biot Elastic Constant	0.8	0.7	0.75	0.7	0.7	0.85
Permeability [in^2]	1.5E-10	1.5E-10	1.5E-10	1.5E-10	1.5E-10	1.5E-10
Porosity [%]	17	16	14	10	10	18
Fluid Specific Weight [Ib/in^3]	0.0367	0.0367	0.0483	0.0367	0.0367	0.0375
Fluid Bulk modulus [psi]	250000	250000	250000	250000	250000	250000
Grain Bulk modulus [psi]	8057368	5371579	7578054	9668842	9668842	16114737

Table 1. Input Data for Two Models.

Case	Impermeable Borehole Wall Total Deformation Area [in^2]			Permeable Borehole Wall Total Deformation Area [in^2]		
	Analytical Results	Numerical Results	Relative Error %	Analytical Results	Numerical Results	Relative Error %
1	0.0161	0.0183	14	0.0111	0.0126	14
2	-0.1045	-0.0978	6	-0.1111	-0.1042	6
3	-0.0467	-0.0538	15	-0.0598	-0.0688	15
4	0.0536	0.0572	7	0.0411	0.0374	9
5	-0.3369	-0.3257	3	-0.3494	-0.3611	3
6	-0.1585	-0.1345	15	-0.1685	-0.1512	10

Table 2. Results and Comparisons.

5 Sensitivity Study on Elastic Deformation of the Open Borehole

The main task of the present study is to individually pinpoint the influences of different parameters on elastic deformation of the open borehole, nine parameters have been examined. The data used for the current study here is synthetic data and was carefully selected. Table 3 shows the parameters with base case data and the other relevant data required to perform the work.

Borehole inclination and orientation are used instead of the stresses to determine the impacts of the far-field principle stresses, therefore the stress transformation equations have to be used to compute the actual applied stresses in the borehole coordinate system whenever azimuth and inclination has been changed. In total nine cases will be studied, for the sake of this sensitivity study, one parameter is allowed to be changed each time whereas the others are frozen. Allowable variation from the base case for each parameter is set to be between -20% to 20%.

Proposed general solutions for computing the radial elastic displacements in permeable borehole wall is used to estimate the deformation area for each case .Because the layer thickness is assumed to be one feet, therefore the deformation volume is equal to the estimated deformation area. The drilling fluid temperature was selected to be 113.4^0 C for the base case so that the effect of the thermal stress can be eliminated.

Parameter	Value
Main data	
Young's Modulus [psi]	2900653
Poisson's Ratio	0.35
Biot Elastic Constant	0.8
Formation Pore Pressure [psi/ft]	0.5
Drilling Fluid Temperature [^{0}C]	113.4
Inclination [^{0}]	18
Azimuth [^{0}]	18
Borehole Radius [in]	6.125
Borehole Pressure [psi/ft]	0.983
Relevant data	
Depth [ft]	12000
Thermal Gradient [^{0}C/ft]	0.00945
Thermal Expansion Coefficient [1/ ^{0}C]	0.000012
Vertical l Stress Gradient [psi/ft]	1.2
Max Horizontal Gradient Stress [psi/ft]	0.97
Min Horizontal Gradient Stress [psi/ft]	0.85

Table 3: The Base Case and the Relevant Data Used for the Study.

5.1 Results and Discussion

The results of the study are graphically presented in Fig. 7. From Fig. 7 it is observed that the deformation volume is directly proportional to borehole pressure, Poisson's ratio, formation pore pressure and Biot elastic constant and it is inversely proportional to the drilling fluid temperature and inclination. In addition it is obvious that a change in Young's modulus, wellbore radius or azimuth would slightly change the magnitude of the deformation but not the status of the borehole [From expansion to contraction or vice versa]. These observations are logical and foreseeable and can be scientifically explained.

Borehole pressure:
An increase in the borehole pressure certainly would cause the borehole to expand as long as no change occurs to the initial status of the in situ stresses.

Formation pore pressure and Biot elastic constant:
These two parameters have direct influence on the effective stresses. Any change in one of them will cause immediate change to the magnitude of the effective stresses. Any increase in one of them will cause immediate decrease to the magnitude of the effective stresses and consequently an expansion to the borehole is anticipated.

Poisson's ratio:
In a real situation two of the rock properties would not change independently Poisson's ratio and Young's modulus. However to satisfy the objective of this study we treat them individually. As it is well known, the in-situ stresses are related to one another. This means that as the axial stress squeezes the rock vertically, it also pushes the rock horizontally, affecting the horizontal stresses which may be constrained by surrounding rocks. The amount of resulting horizontal stress depends largely upon the Poisson's ratio. Therefore if the Poisson's ratio is allowed to increase without changing the magnitude of the stresses the effect of the borehole pressure will be higher on the rock causing the borehole to expand.

Drilling fluid temperature:
Thermal stress mainly is induced by the difference in temperature between the drilling fluid temperature and the formation temperature especially at high temperature high pressure wells. If the difference in temperature is considerably high, the resultant thermal stress will be high likewise; causing an enormous increase in tangential and axial stresses consequently a contraction to the borehole is anticipated.

Inclination:
According to transformation formulas any increase in the borehole inclination will result in an increase to the horizontal stresses which in turn will increase the local effective stresses and according to that borehole will shrink.

Young's modulus, wellbore radius and azimuth:
Based on the data used for the present study the effect of these three variables on the deformation is incommodious and they cannot change the status of the borehole independently. As it can be seen in Fig. 7, the deformation volume for the base case is negative indicating a contraction status which will never be changed even with increase or decrease these parameters. Therefore Young's modulus, wellbore radius and azimuth cannot be the main dominator in the cases when they are allowed to change with freezing the other parameters.

Other important observation which can be extracted from the study is that the deformation area of the borehole due to the elastic deformation is not significant and it does not exceed quarter inches square in worst cases.

Based on the aforementioned discussion the parameters which have impact on the deformation volume of an open borehole, can be classified based on different aspects. The flowchart below [Fig. 8] clearly illustrates the hierarchy of proposed classification by the authors.

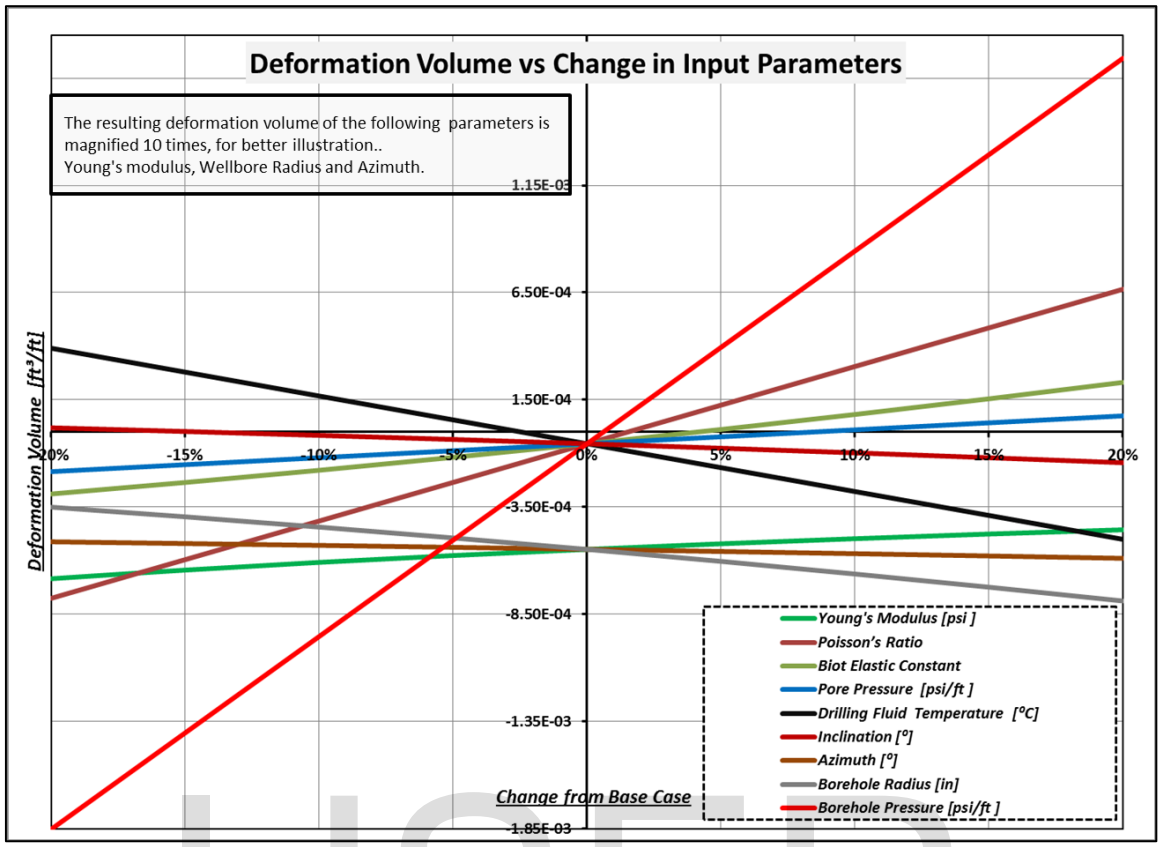

Fig 7. Variation in the Deformation Volume for Different Cases.

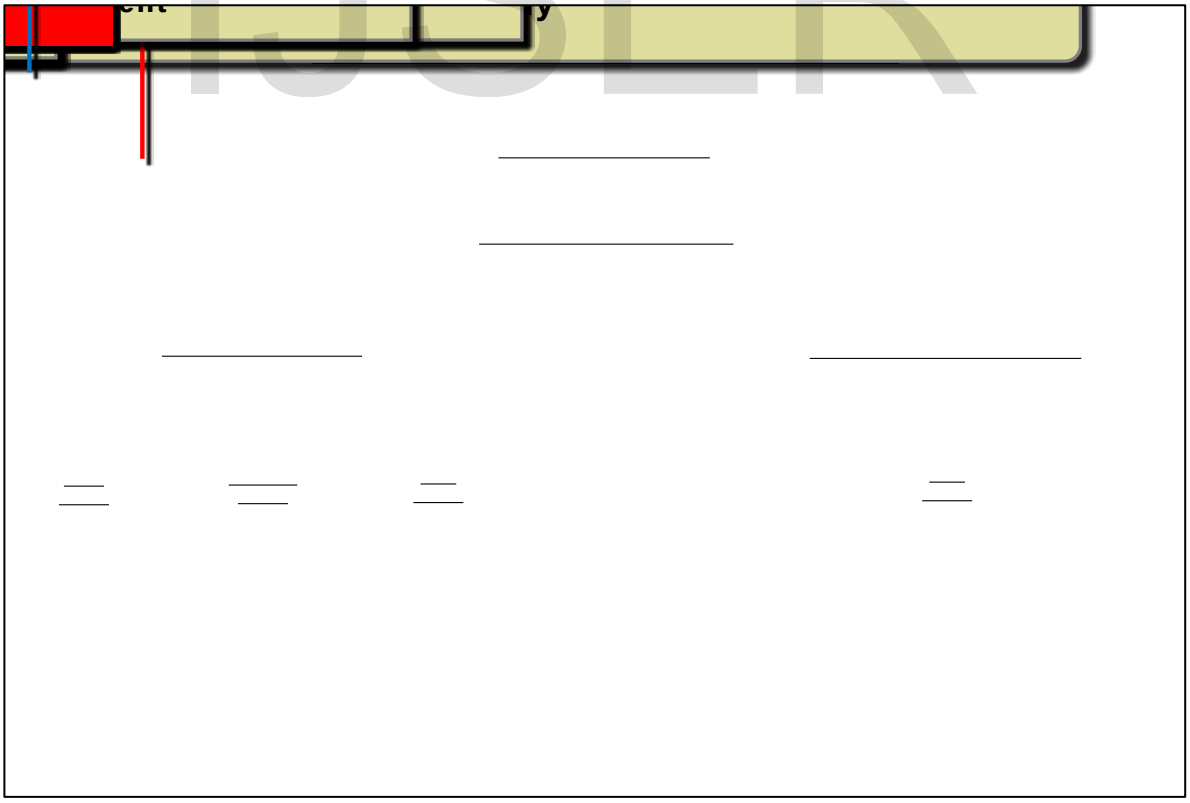

Fig 8. Hierarchy of Proposed Classification.

6 CONCLUSIONS

The main conclusion of the presented work can be summarized in the following points:

- The analytical formulations proposed in this paper for estimating the radial elastic displacement of the open borehole wall give reasonably accurate results as indicated by the relative error shown in validation section; in addition they take into account the factors which have not been considered formerly.
- Recognized mathematical methods have been adapted to estimate the deformation area for a given depth.
- Practical concept to determine the volumetric change of an open borehole has been comprehensively described.
- Practically, the impermeable proposed solution is valid once the rock formation is exposed to the drilling fluid and last as long as no filtration occurs [Initial condition], whereas the permeable solution is effective only when a stable mud cake is built [Steady stat condition].
- Alternate models to investigate the radial elastic displacement of an open borehole using ABAQUS are presented.
- Estimation of volumetric change induced by expansion and contraction of natural and induced fractures is not an easy task and has high uncertainty due to the lack of accurate data such as the number of active fractures and the interconnection between the existing fractures; however having a concrete idea about the elastic deformation of the borehole wall besides the thermal expansion and the compressibility of the drilling fluid would assist to improve the estimation quality by reducing the uncertainty.
- The sensitivity study demonstrates that the volumetric change of the borehole due to the elastic deformation;
  - Is volatile and mainly controlled by the drilling fluid weight and temperature.
  - Is not significant when taken into account individually.

7. ACKNOWLEDGMENT

The authors would like to disclose gratitude to the Chair of Drilling and Completion Engineering from the Montanuniversität Leoben, Austria.

8. CONFLICTS OF INTEREST

The author(s) declare(s) that there is no conflict of interest regarding the publication of this manuscript.

9 NOMENCLATURES

σ	Normal stress
ε	Normal strain
E	Young's modulus
σ_x	Far field principle stress in [x] axis
σ_y	Far field principle stress in [y] axis
σ_z	Far field principle stress in [z] axis
ε_x	Principle strain in [x] axis
ε_y	Principle strain in [y] axis
ε_z	Principle strain in [z] axis
υ	Poisson ratio
σ_r	Radial stress
σ_θ	Tangential stress
σ_z	Stress along the borehole axis
ε_r	Radial strain
ε_θ	Tangential strain
ε_z	Strain along the borehole axis
r	Wellbore radius
u	Radial elastic displacement for the borehole
σ_x°	Transformed stress in in [x] axis
σ_y°	Transformed stress in in [y] axis
σ_z°	Transformed stress in in [z] axis
τ_{xy}°	Shear stresses in [x,y] plane
τ_{yz}°	Shear stresses in [y,z] plane
σ_H	Maximum horizontal principle stress
σ_h	Minimum horizontal principle stress

σ_v	Vertical principle stress
ω	Borehole azimuth
δ	Borehole inclination
R	Arbitrary radius
θ	Angle around the borehole measured anticlockwise from the azimuth of σ_H
σ_{rr}	Effective radial stress
$\sigma_{\theta\theta}$	Effective tangential stress
σ_{zz}	Effective stress along the borehole axis
$\tau_{\theta z}$	Shear stresse in [θ,z] plane
$\sigma_t^{\Delta t}$	Thermal stress
α_t	Thermal expansion coefficient
T_i	Original formation temperature
T_w	Drilling fluid temperature
P_w	Borehole Pressure
P_p	Formation pore pressure
α	Biot's elastic constant
η	Poroelastic stress coefficient
$\emptyset$	Porosity

10 REFERENCES

[1]. Lavrov, A. and Tronvoll, J. 2005. Mechanics of Borehole Ballooning in Naturally-Fractured Formations. Presented at the SPE Middle East Oil & Gas Show and Conference, Bahrain, 12-15 March 2005. SPE-93747-MS.

[2]. Eirik, K. 1998. Analysis of Ballooning Effects During Drilling of High Pressure High Temperature Wells. Presented at SPE European Petroleum Conference, Hague, The Netherlands, 20-22 October 1998. SPE-52066-STU.

[3]. Ozdemirtas, M. Babadagli, T. and Kuru, E. 2007. Numerical Modelling of Borehole Ballooning/Breathing Effect of Fracture Roughness. Presented at the Petroleum Society's 8th Canadian International petroleum Conference (58th Annual Technical Meeting), Calgary, Alberta, Canada, 12-14 June 2007. PETSOC-2007-038.

[4]. Aadnøy, S. and Brent, S. 2010. Evaluation of ballooning in deep wells. In Modern Well Design, second edition, Appendix B, 294. London, Uk: Taylor & Francis Group.

[5]. Helstrup, A. Rahman, M.K. Hossain, M.M. and Rahman, S. 2001. A Practical Method for Evaluating Effects of Fracture Charging and/or Ballooning When Drilling High Pressure, High Temperature (HPHT) Wells. Presented at SPE/IADC Drilling Conference, Netherlands, Amsterdam, 27 February-1 March 2001. SPE-67780-MS.

[6]. Tahini, AL. Ashraf, M. Abousleiman. and Younane, N. 2008. Insights into borehole deformation and relationship between wellbore induced stresses, breakouts, and in-situ stresses. Presented at San Francisco 2008, the 42nd US Rock Mechanics Symposium and 2nd U.S,Canada Rock Mechanics Symposium, San Francisco, 29June-2July 2008. ARMA-08-037.

[7]. Aadnøy, S. and Looyeh, R. 2011. Stresses Around A Wellbore. In Petroleum Rock Mechanics Drilling Operations And Well Design, first edition, Chapter10,157: Gulf Professional Publishing is an imprint of Elsevier.

[8]. Peng, S. and Zhang, J. 2007. Wellbore/borehole stability. In Engineering Geology for nderground Rocks, first edition, Chapter7,169. Berlin, Germany: Springer Science and Business Media.

[9]. Fjær, E. Holt, R.M. Horsrud, P. Raaen, A.M. and Risnes, R. 2008. Stresses around boreholes. Borehole failure criteria. In Petroleum Related Rock Mechanics, second edition, Chapter4,146,157. Amsterdam, the Netherlands: Elsevier B.V.

[10]. Wikipedia.2015. https://en.wikipedia.org/wiki/Riemann_sum.

[11]. Klimentos, T. Harouaka, A. Mtawaa, B. and Saner, S. 1998. Experimental Determination of the Biot Elastic Constant: Applications in Formation Evaluation (Sonic Porosity, Rock Strength, Earth Stresses, and Sanding Predictions). SPE Reservoir Evaluation & Engineering. SPE-30593-PA.

[12]. Farrokhrouz, M. and Asef, M. Evaluation of Empirical Correlations for Biot's Coefficient Prediction. ResearchGate.

[13]. Reza, K. and Sajad, J. Building a Mechanical Earth Model and its Application in a Geomechanical Analysis of Hydraulic Fracture Behaviour in Naturally Fractured Reservoirs. European Journal of Environmental and Civil Engineering. Vol. 18, No. 3, 336 – 357, November 2013.

[14]. Yonglai, Z. and Shuxin, D. Failure Probability Model considering the Effect of Intermediate Principal Stress on Rock Strength. Hindawi Publishing Corporation, Journal of Mathematical Problems in Engineering, Volume 2015, Article ID 960973, 7 pages, November 2015.

[15]. Titus, N. Sonny, I. and William, P. CFD Method for Predicting Annular Pressure Losses and Cuttings

Concentration in Eccentric Horizontal Wells. Hindawi Publishing Corporation, Journal of Petroleum Engineering, Volume 2014, Article ID 486423, 16 pages, April 2014.

11 APPENDIX A

By Breaking down Eq. 4 we get:

$$\varepsilon_r = \frac{1}{E}[\sigma_r - (\upsilon * \sigma_\theta) - (\upsilon * \sigma_z)] \quad (A1)$$

$$\varepsilon_\theta = \frac{1}{E}[\sigma_\theta - (\upsilon * \sigma_r) - (\upsilon * \sigma_z)] \quad (A2)$$

$$\varepsilon_z = \frac{1}{E}[\sigma_z - \upsilon * \sigma_\theta - \upsilon * \sigma_r] \quad (A3)$$

Because the borehole can be either vertical or deviated, therefore it is necessary to utilize stress transformation Equations in order to compute the stresses in the borehole coordinate system.

$$\sigma_x^\circ = \left(\sigma_H * \left(\mathrm{COS}(\omega)\right)^2 + \sigma_h * \left(\mathrm{SIN}(\omega)\right)^2\right) * \left(\mathrm{COS}(\delta)\right)^2 + \sigma_v * \left(\mathrm{SIN}(\delta)\right)^2 \quad (A4)$$

$$\sigma_y^\circ = \left(\sigma_H * \left(\mathrm{SIN}(\omega)\right)^2 + \sigma_h * \left(\mathrm{COS}(\omega)\right)^2\right) \quad (A5)$$

$$\sigma_z^\circ = \left(\sigma_H * \left(\mathrm{COS}(\omega)\right)^2 + \sigma_h * \left(\mathrm{SIN}(\omega)\right)^2\right) * \left(\mathrm{SIN}(\delta)\right)^2 + \sigma_v * \left(\mathrm{COS}(\delta)\right)^2 \quad (A6)$$

$$\tau_{xy}^\circ = \frac{1}{2}(\sigma_H - \sigma_h) * \left(\mathrm{SIN}(2\omega)\right) * \left(\mathrm{COS}(\delta)\right) \quad (A7)$$

$$\tau_{xz}^\circ = \frac{1}{2}\left(\sigma_H * \left(\mathrm{COS}(\omega)\right)^2 + \sigma_h * \left(\mathrm{SIN}(\omega)\right)^2 - \sigma_v\right) * \left(\mathrm{SIN}(2\delta)\right) \quad (A8)$$

$$\tau_{yz}^\circ = \frac{1}{2}(\sigma_H - \sigma_h) * \left(\mathrm{SIN}(2\omega)\right) * \left(\mathrm{SIN}(\delta)\right) \quad (A9)$$

σ_H , σ_h, σ_v , τ_{xy}, τ_{xz} and τ_{yz} will be used instead of σ_x°, σ_y°, τ_{xy}°, τ_{xz}° and τ_{yz}° respectively.

The stress distribution around a borehole located in an arbitrary far-field stress field according to Bradley (1979) can be computed by the following equations:

$$\sigma_r = \frac{1}{2}(\sigma_H + \sigma_h)\left(1 - \frac{R^2}{r^2}\right) + \frac{1}{2}(\sigma_H - \sigma_h)\left(1 + 3\frac{R^4}{r^4} - 4\frac{R^2}{r^2}\right)\mathrm{COS}(2\theta) + \tau_{xy}\left(1 + 3\frac{R^4}{r^4} - 4\frac{R^2}{r^2}\right)\mathrm{SIN}(2\theta) + P_w\frac{R^2}{r^2} \quad (A10)$$

$$\sigma_\theta = \frac{1}{2}(\sigma_H + \sigma_h)\left(1 + \frac{R^2}{r^2}\right) - \frac{1}{2}(\sigma_H - \sigma_h)\left(1 + 3\frac{R^4}{r^4}\right)\mathrm{COS}(2\theta) - \tau_{xy}\left(1 + 3\frac{R^4}{r^4}\right)\mathrm{SIN}(2\theta) - P_w\frac{R^2}{r^2} \quad (A11)$$

$$\sigma_z = \sigma_v - 2 * \upsilon(\sigma_H - \sigma_h) * \frac{R^2}{r^2}\mathrm{COS}(2\theta) - 4 * \upsilon * \tau_{xy}\frac{R^2}{r^2}\mathrm{SIN}(2\theta) \quad (A12)$$

$$\tau_{\theta z} = \left(\tau_{yz} * \mathrm{COS}(\theta) - \tau_{xz} * \mathrm{SIN}(\theta)\right)\left(1 + \frac{R^2}{r^2}\right) \quad (A13)$$

Applying the advanced assumptions and considerations to Eq. A10 to A13;

$$\sigma_{rr} = P_w - \left(\alpha * P_p\right) \quad (A14)$$

$$\sigma_{\theta\theta} = (\sigma_H + \sigma_h) - P_w - \left(\alpha * P_p\right) + \sigma_t^{\Delta t} - 2 * (\sigma_H - \sigma_h)\,\mathrm{COS}(2\theta) - 4 * \tau_{xy} * \mathrm{SIN}(2\theta) \quad (A15)$$

$$\sigma_{zz} = \sigma_v - \left(\alpha * P_p\right) + \sigma_t^{\Delta t} - 2 * \upsilon(\sigma_H - \sigma_h)\,\mathrm{COS}(2\theta) - 4 * \upsilon * \tau_{xy} * \mathrm{SIN}(2\theta) \quad (A16)$$

$$\tau_{\theta z} = 2 * \left(\tau_{yz} * \mathrm{COS}(\theta) - \tau_{xz} * \mathrm{SIN}(\theta)\right) \quad (A17)$$

$$\sigma_t^{\Delta t} = \frac{E.\alpha_t}{(1 - v)}(T_w - T_i) \quad (A18)$$

Back to Eq. A2, substituting σ_r, σ_θ and σ_z in Eq. A2 with the effective stresses Eq. A14, A15 and A16 respectively, the tangential strain equation will be:

$$\varepsilon_\theta = \frac{1}{E}[\left((\sigma_H + \sigma_h) - P_w - \left(\alpha * P_p\right) + \sigma_t^{\Delta t} - 2 * (\sigma_H - \sigma_h)\,\mathrm{COS}(2\theta) - 4 * \tau_{xy} * \mathrm{SIN}(2\theta)\right) - \upsilon * \left(P_w - \left(\alpha * P_p\right)\right) - \upsilon * \left(\sigma_v - \left(\alpha * P_p\right) + \sigma_t^{\Delta t} - 2 * \upsilon(\sigma_H - \sigma_h)\,\mathrm{COS}(2\theta) - 4 * \upsilon * \tau_{xy} * \mathrm{SIN}(2\theta)\right) \quad (A19)$$

After few mathematical steps and arrangements, the equation will have the following final form;

$$\varepsilon_\theta = \frac{(1 + \upsilon)}{E}\left[\frac{(2\upsilon - 1)}{(1 + \upsilon)} * \left(\alpha * P_p\right) - P_w + \frac{(1 - \upsilon)}{(1 + \upsilon)} * \sigma_t^{\Delta t} + \frac{1}{(1 + \upsilon)} * (\sigma_H + \sigma_h - \upsilon * \sigma_v) + 2 * (\upsilon - 1) * \left((\sigma_H - \sigma_h)\,\mathrm{COS}(2\theta) + 2 * \tau_{xy} * \mathrm{SIN}(2\theta)\right)\right] \quad (A20)$$

Finally we obtain the first proposed analytic solution for computing the radial displacement of the impermeable borehole wall by replacing ε_θ in Eq. 09 with Eq. A20.

$$u = r * \frac{(1+\upsilon)}{E}\left[P_w - \frac{(2\upsilon-1)}{(1+\upsilon)} * (\alpha * P_p) - \frac{(1-\upsilon)}{(1+\upsilon)} * \sigma_t^{\Delta t} - \frac{1}{(1+\upsilon)} * (\sigma_H + \sigma_h - \upsilon * \sigma_v) - 2 * (\upsilon - 1) * \left((\sigma_H - \sigma_h)\,COS(2\theta) + 2 * \tau_{xy} * SIN(2\theta)\right)\right] \quad (A21)$$

12 Appendix B

$$\sigma_{rr} = P_w(1-\alpha) \quad (B1)$$

$$\sigma_{\theta\theta} = (\sigma_H + \sigma_h) - P_w(1+\alpha) + \sigma_t^{\Delta t} - 2 * (\sigma_H - \sigma_h)\,COS(2\theta) - 4 * \tau_{xy} * SIN(2\theta) + 2\eta\left(P_w - (\alpha * P_p)\right) \quad (B2)$$

$$\sigma_{zz} = \sigma_v - (\alpha * P_w) + \sigma_t^{\Delta t} - 2 * \upsilon(\sigma_H - \sigma_h)\,COS(2\theta) - 4 * \upsilon * \tau_{xy} * SIN(2\theta) + 2\eta\left(P_w - (\alpha * P_p)\right) \quad (B3)$$

$$\eta = \frac{\alpha(1-2\upsilon)}{2(1-\upsilon)} \quad (B4)$$

By substituting σ_r, σ_θ and σ_z in Eq. A2 with the effective stresses Eq. B1, B2 and B3 respectively, the tangential strain equation finally will be:

$$\varepsilon_\theta = \frac{1}{E}\left[(\alpha * P_w) * (2\upsilon - 1) - P_w * (1+\upsilon) + (1-\upsilon) * \left(\sigma_t^{\Delta t} + 2\eta\left(P_w - (\alpha * P_p)\right)\right) + (\upsilon^2 - 1) * \left(2(\sigma_H - \sigma_h)\,COS(2\theta) + 4 * \tau_{xy} * SIN(2\theta)\right) + \sigma_H + \sigma_h - \upsilon * \sigma_v\right] \quad (B5)$$

The second proposed analytic solution for computing the radial elastic displacement of the permeable borehole wall is obtained by replacing ε_θ in Eq. 09 with Eq. B5.

$$u = r * \frac{1}{E}\left[P_w * (1+\upsilon) - (\alpha * P_w) * (2\upsilon - 1) - (1-\upsilon) * \left(\sigma_t^{\Delta t} + 2\eta\left(P_w - (\alpha * P_p)\right)\right) - (\upsilon^2 - 1) * \left(2(\sigma_H - \sigma_h)\,COS(2\theta) + 4 * \tau_{xy} * SIN(2\theta)\right) - \sigma_H - \sigma_h + \upsilon * \sigma_v\right] \quad (B6)$$

13 Appendix C

Krief et al. (1990): $$\boldsymbol{\alpha = 1 - (1-\emptyset)^{\frac{3}{1-\emptyset}}} \quad (\boldsymbol{C1})$$

Lee (2002): $$\alpha = 0.98469 + \frac{-68.7421}{1 + e^{\frac{\emptyset + 0.40635}{0.09425}}} \quad (C2)$$

Laurent et al. (1993): $$\alpha = 1.75 * \emptyset^{0.51} \quad (C3)$$

Wang et al. (2001): $$\alpha = 1 - e^{(-3.8*\emptyset - 0.86)} \quad (C4)$$

Dip. Ing. Asad Elmgerbi, Phd student, Montanuniversität Leoben (MUL), Department of Petroleum Engineering (DPE), Chair of Drilling and Completion Engineering (CDC), Max-Tendler-Straße 4, 8700, Leoben, Austria.
Univ.-Prof. Dipl.-Ing. Dr.mont Gerhard Thonhauser, Head of Petroleum Engineering Department, Montanuniversität Leoben (MUL), Department of Petroleum Engineering (DPE), Chair of Drilling and Completion Engineering (CDC), Max-Tendler-Straße 4, 8700, Leoben, Austria.
Ass.Prof. Dipl.-Ing. Dr.mont. Michael Prohaska, Montanuniversität Leoben (MUL), Department of Petroleum Engineering (DPE), Chair of Drilling and Completion Engineering (CDC), Max-Tendler-Straße 4, 8700, Leoben, Austria.
Abbas Roohi, Montanuniversität Leoben (MUL), Department of Petroleum Engineering (DPE), Chair of Drilling and Completion Engineering (CDC), Max-Tendler-Straße 4, 8700, Leoben, Austria.
Dip. Ing. Andreas Nascimento, Universidade Estadual Paulista (UNESP), Faculdade de Engenharia, Câmpus de Guaratinguetá (FEG), Departamento de Mecânica (DME)/PRH48-ANP, Avenida Ariberto Pereira da Cunha 333, Portal das Colinas, 12.516-410 Guaratinguetá, SP, Brazil